

## Research Article

# Breast Cancer Classification from Mammogram Images Using Extreme Learning Machine-Based DenseNet121 Model

Raj Kumar Pattanaik,<sup>1</sup> Satyasis Mishra,<sup>2</sup> Mohammed Siddique,<sup>1</sup>  
Tiruvedula Gopikrishna ,<sup>3</sup> and Sunita Satapathy<sup>4</sup>

<sup>1</sup>Department of Mathematics, Centurion University of Technology and Management, Odisha, India

<sup>2</sup>Department of ECE, Centurion University of Technology and Management, Odisha, India

<sup>3</sup>Department of CSE, Adama Science and Technology University, Adama, Ethiopia

<sup>4</sup>Department of Zoology, Centurion University of Technology and Management, Odisha, India

Correspondence should be addressed to Tiruvedula Gopikrishna; [gktiruvedula@gmail.com](mailto:gktiruvedula@gmail.com)

Received 11 October 2022; Revised 8 December 2022; Accepted 12 December 2022; Published 31 December 2022

Academic Editor: Giorgio Pennazza

Copyright © 2022 Raj Kumar Pattanaik et al. This is an open access article distributed under the Creative Commons Attribution License, which permits unrestricted use, distribution, and reproduction in any medium, provided the original work is properly cited.

Breast cancer is characterized by abnormal discontinuities in the lining cells of a woman's milk duct. Large numbers of women die from breast cancer as a result of developing symptoms in the milk ducts. If the diagnosis is made early, the death rates can be decreased. For radiologists and physicians, manually analyzing mammography images for breast cancer become time-consuming. To prevent manual analysis and simplify the work of classification, this paper introduces a novel hybrid DenseNet121-based Extreme Learning Machine Model (ELM) for classifying breast cancer from mammogram images. The mammogram images were processed through preprocessing and data augmentation phase. The features were collected separately after the pooling and flatten layer at the first stage of the classification. Further, the features are fed as input to the proposed DenseNet121-ELM model's fully connected layer as input. An extreme learning machine model has replaced the fully connected layer. The weights of the extreme learning machine have been updated by the AdaGrad optimization algorithm to increase the model's robustness and performance. Due to its faster convergence speed than other optimization techniques, the AdaGrad algorithm optimization was chosen. In this research, the Digital Database for Screening Mammography (DDSM) dataset mammogram images were utilized, and the results are presented. We have considered the batch size of 32, 64, and 128 for the performance measure, accuracy, sensitivity, specificity, and computational time. The proposed DenseNet121+ELM model achieves 99.47% and 99.14% as training accuracy and testing accuracy for batch size 128. Also, it achieves specificity, sensitivity, and computational time of 99.37%, 99.94%, and 159.7731 minutes, respectively. Further, the comparison result of performance measures is presented for batch sizes 32, 64, and 128 to show the robustness of the proposed DenseNet121+ELM model. The automatic classification performance of the DenseNet121+ELM model has much potential to be applied to the clinical diagnosis of breast cancer.

## 1. Introduction

Breast cancer is the uncontrolled growth of breast tissue. Breast cancer accounts for 12.5% of all new cancer cases each year, making it the most prevalent cancer in the world. About 30% of newly diagnosed malignancies in women are predicted to be breast cancers in 2022. Being a woman and getting older are the two most significant risk factors for breast cancer. The biggest global public health issue right

now is cancer. According to the WHO (World Health Organization), IARC (International Agency for Research on Cancer), and the GBD (Global Burden of Disease Cancer Collaboration), they say that the cases of cancer have risen 28 percent from 2006 to 2010 and there will be 2.7 million new cases of cancer in 2030. Breast cancer affects more women than any other type of cancer (1.7 million incidents, 535,000 deaths, and 14.9 million life years adjusted for people with disabilities). The incidence and mortality rates of

breast cancer have shown enduring inequities, according to the American Cancer Society. The American Cancer Society (ACS) research states that in 2022, breast cancer will be a major cause of high-mortality rates [1]. The report estimates a daily death toll of 1,670. Invasive breast cancer will affect roughly 13% (or 1 in 8) of American women during their lifetime. Breast cancer treatment at its early stage becomes an essential part of the diagnosis. There is also a highly significant diagnosis of breast cancer early on in order to improve the survival rate. Breast cancer diagnosis by manual intervention consumes lots of time to understand and classify from the mammogram images. In recent years, deep learning algorithms like CNN have proved their capability to detect breast cancers from pathological images. It was also found that some models failed due to overfitting. We believe this complex diagnosis system can be made more accessible by designing an automated deep-learning classification system. Motivated by the advancement of deep learning, we have developed a novel classification model for the classification of breast cancer. The development of deep learning as an image classification technique is crucial in the current research era. Several studies proposed classifying mammography images, and the effectiveness of the classifiers was demonstrated using binary, multi, and dual classification. By randomly deleting layers from CNN models during training, deep learning significantly enhances the training of deep networks [2]. The MobileNets are built using a productive architecture that creates deep neural networks using depth-wise convolutions [3]. ResNet was suggested by Xie et al. [4] for image classification. With a training accuracy of 98%, Falconi et al. [5] recommended VGG, Xception, and ResNet for the classification of breast cancer. DenseNet and SENet were suggested by Li et al. [6] to be interleaved with histological images for the classification of breast cancer. With five-folder cross-validation, Wang et al. [7] proposed modified InceptionV3 architecture and achieved an area under the curve (AUC) value of 0.9468, sensitivity, and specificity of 0.886 and 0.876, respectively. With the MIAS dataset, Shin et al. [8] proposed Multiscale All Convolutional Neural Network (MA-CNN) and achieved a sensitivity of 96% and 0.99 AUC. Squeeze-Excitation-Pruning (SEP) block for histopathology images for breast cancer classification was suggested by Zhu et al. [9] in their hybrid CNN architecture. After a thorough review of the literature, it was found that there was no research on the use of the DenseNet121+ELM model for mammography images. Due to the lack of faster-performance conventional CNN automatic classifiers, we are inspired to propose the DenseNet121-ELM model. The proposed model performs well when compared to the existing CNN models for classification.

The contributions are as follows:

- (i) We developed DenseNet121 model hybridization with an extreme learning machine (ELM) at fully connected layer
- (ii) We proposed an extreme learning machine (ELM) model after the flattened layer for classification
- (iii) We have utilized AdaGrad optimization for the weight optimization of the model with a batch size of 32, 64, and 128

The remaining sections are organized as follows: the related research done by researchers is presented in Section 2, the methodology, the research diagram, and the architecture of the proposed DenseNet121+ELM models are presented in Section 3, the results and discussion are presented in Section 4, and the conclusion and references are presented in Section 5.

## 2. Related Works

On the basis of medical imaging, researchers from all around the world are developing techniques for automatic breast cancer identification and classification. Due to the rapid growth of deep learning in the medical imaging field, the researchers are attracted towards this new research. The essential element of any diagnostic system is that it aids radiologists and medical professionals in the early identification of cancer. For breast cancer, various deep learning-based classification algorithms were developed. Shear-wave elastography (SWE) data and CNN were combined with a segmentation-free radiomics technique for breast tumor classification proposed by Zhou et al. [10]. For feature extraction, this approach produced elastic morphology data. For the suggested experiment, 318 malignant breast tumors and 222 benign breast tumors were used. During the final experiment, the suggested SWE-CNN model achieved specificity of 95.7%, sensitivity of 96.2%, and accuracy of 95.8%. Mask regions with CNN were suggested by Chiao et al. [11] for the classification of breast cancer from CT scan images. The data was collected from China Medical University Hospital using ultrasound images together with biopsy, histology, and diagnostic reports. For the experiment, a total of 307 ultrasound images from 80 instances were gathered. They have achieved an overall accuracy of 85% in diagnosing benign and malignant breast tumors using the proposed Mask R-CNN. A compact SE-ResNet module for the CNN classifier was suggested by Jiang et al. [12] in order to enhance CNN performance with fewer parameters. The CNN's squeeze-and-excitation block and residual module are combined to form the SE-ResNet. The research employed the BreakHis dataset, which has an accuracy rate of 98.87% for binary classification and 93.81% for multiclass classification. A deep learning architecture with transfer learning was presented by Khan et al. [13] for the classification of breast cancer in breast cytology images. The LRH hospital in Peshawar, Pakistan, provided the histopathology dataset. The GoogLeNet, Visual Geometry Group Network (VGGNet), and Residual Networks (ResNet) were utilized for feature extraction. The combined features were then given to the fully connected layer with average pooling for the classification of cancerous and benign cells. The accuracy of the proposed deep learning framework was 97.525%. The deep learning Xception model for breast cancer classification was proposed by

Abunasser et al. [14]. The research used 7909 microscopic images from the BreakHis breast cancer dataset, which included 2,480 benign and 5,429 malignant samples. The proposed Xception model attained training accuracy, precision, recall, and F1-score of 99.78%, 97.60%, and 97.58%, respectively. A hybrid improved marine predators algorithm- (IMPA-) ResNet50 model and transfer learning were proposed by Houssein et al. in 2022 [15]. The optimum hyperparameters of the CNN architecture were identified using the IMPA. For experimentation, the DDSM dataset and the MIAS dataset were employed. The MIAS dataset achieved 98.88% accuracy, 97.61% sensitivity, and 98.40% specificity for the classification of breast cancer, while the DDSM and earned an accuracy of 98.32%, 98.56% sensitivity, and 98.68%. The DenseNet CNN model was proposed by Nawaz et al. [16] for the multiclass classification of breast cancer and predicted the subclass of cancers like fibroadenoma and lobular carcinoma. DenseNet CNN model produced outstanding processing results with 95.4% accuracy using the histopathology BreakHis image dataset. Khan et al. [17] proposed deep CNN ResNet50 model to segment and classify types of breast abnormalities into benign and malignant cases. The proposed model has reached 88% accuracy in classifying breast cancer abnormalities such as masses, calcifications, carcinomas, and asymmetry mammograms. In order to distinguish between normal tissue and benign lesions in hematoxylin-eosin-stained breast cancer microscopy images, Hameed et al. [18] proposed Xception with six intermediate layers. The classification proposal made by the Xception model makes use of its own layering structure. The performance of the model was investigated on four normalized datasets resulting from Reinhard, Ruifrok, Macenko, and Vahadane stain normalization. They employed  $5 \times 5$  cross-validation for the performance measure and achieved 97.79% accuracy with a kappa value of  $0.965$ . Hu moment, Haralick textures, color histogram feature extraction techniques, and a DNN classifier were proposed by Joseph et al. [19] for the multiclassification of histopathology images. To prevent overfitting, the DNN employs four dense layers, a softmax function in its structure, and data augmentation. When classifying images using the BreakHis dataset, 97.87% accuracy was attained for  $40 \times$  magnification-dependent histopathological images. In order to enhance the color separation and contrast, Alkassar et al. [20] suggested a magnification-specific binary (MSB) and magnification-specific multcategory (MSM) classification approach that normalizes the hematoxylin and eosin stains. With the BreakHis histopathology dataset, two unique feature types—deep and shallow features— were extracted using two deep DenseNet and Xception structure networks and achieved an accuracy of 99% and 92% in terms of MSB and MSM classification. Altameem et al. [21] proposed an ensemble approach, where the Gompertz function was used to form fuzzy rankings of the base classification. InceptionV4, ResNet-164, VGG-11, and DenseNet121 models were considered as base classifiers. They have used four datasets as DDSM, BCDR, Mini-MIAS, and INbreast. An accuracy rate of 99.32% was achieved by the InceptionV4

model with fuzzy rank-based Gompertz function which was higher than the other ResNet-164, VGG-11, and DenseNet121 base models. Alqhtani [22] proposed a novel layer-based Convolutional Neural Network (BreastCNN) for breast cancer method, which works in five different layers and uses different types of filters. Breast cancer was classified with an accuracy of 99.7% using the Database for Mastology Research (DMR), which contains 745 healthy and 261 sick photos. Hosni Mahmoud et al. [23] proposed a deep CNN method for feature extraction, and the features are coupled along with the texture features for the classification of breast cancer. A support vector machine was trained on deep CNN for classification along with scale-invariant feature transform (SIFT) algorithm and achieved an accuracy of 97.8% with a TP rate of 98.45% and a TN rate of 96%. A hybrid model based on “Pulse-Coupled Neural Networks (PCNNs) and Deep Convolutional Neural Networks (CNNs)” was developed by Altaf [24] using three publically accessible datasets, including the DDSM, INbreast, and BCDR datasets. From the three datasets, they have used 900, 300, and 450 images, respectively. The hybrid PCNN-CNN model attained 98.72%. For the DDSM, INbreast, and BCDR datasets, respectively, accuracy values were 97.5%, 96.94%, and 96.94%. Using a combination of deep neural networks (ResNet 18, ShuffleNet, and InceptionV3Net with 18, 48, and 50 hidden layers) and transfer learning with the BreakHis dataset, Aljuaid et al. [25] proposed a novel CAD method for breast cancer classification and achieved average accuracies of 99.7%, 97.66%, and 96.94% for ResNet, InceptionV3Net, and ShuffleNet, respectively. ResNet, InceptionV3Net, and ShuffleNet each achieved average accuracies of 97.81%, 96.07%, and 95.79% for binary classification and multiclassification, respectively.

### 3. Materials and Methods

*3.1. Research Implementation Diagram.* The research flow diagram in Figure 1(a) presents step-by-step accomplishment of the research work.

*3.2. Proposed DenseNet121+ELM Model and Its Architecture.* The proposed DenseNet121+ELM model architecture is shown in Figure 1(b). After resizing the input mammography images to their original  $224 \times 224$  size, the data was divided into training and testing phases. The dataset is normalized to have a unique dataset and fed to the models VGG19 [26], MobileNet [2], MobileNetV2 [27], Xception [28], ResNet50V2 [28], InceptionV3 [6], InceptionResNetV2 [6], DenseNet201 [29], and DenseNet121 [27]. All the data go through the convolution phases, average pooling, and flatten phases. The models VGG19 [26], MobileNet [2], MobileNetV2 [27], Xception [28], ResNet50V2 [28], InceptionV3 [6], InceptionResNetV2 [6], and DenseNet201 [29] were classify through the conventional phase of the classification through a simple neural network with AdaGrad weight optimization. The DenseNet121 architecture is presented in Figure 2(b).

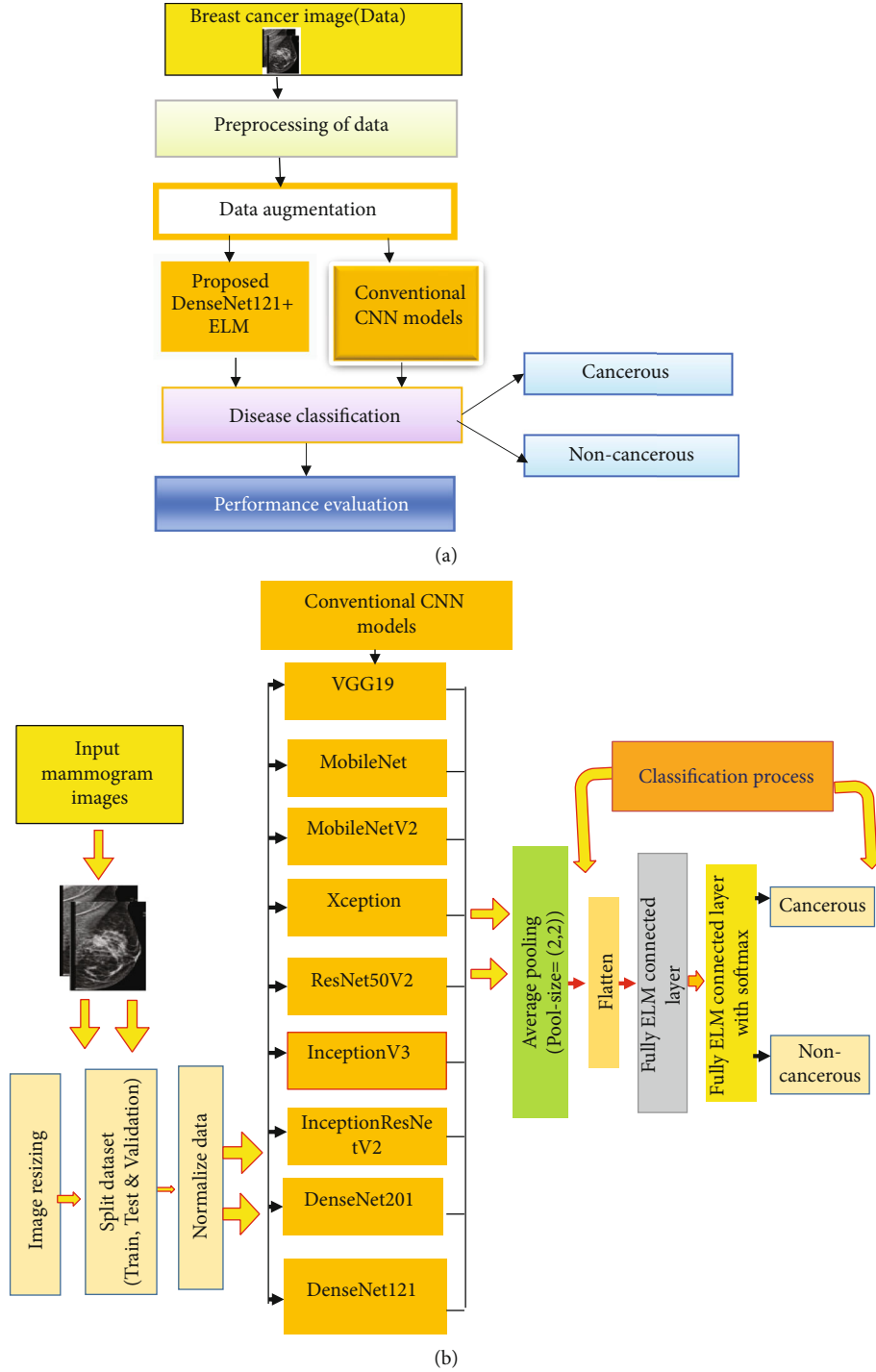


FIGURE 1: (a) Research implementation diagram. (b) Research workflow of proposed DenseNet121+ELM model with comparison CNN models for the classification of breast cancer.

3.2.1. *ELM Model.* The output function of ELM [29] with  $N$  hidden neurons is represented by

$$Y = \sum_{n=0}^N \beta_n g_n(w_n; x) + b_N, \quad (1)$$

where  $g(w; x) = [1, g_1(w_1; x), \dots, g_N(w_N; x)]$  – is the hidden matrix, and  $\beta$  is the weight vector, Equation (1) can be written as

$$H\beta = Y, \quad (2)$$

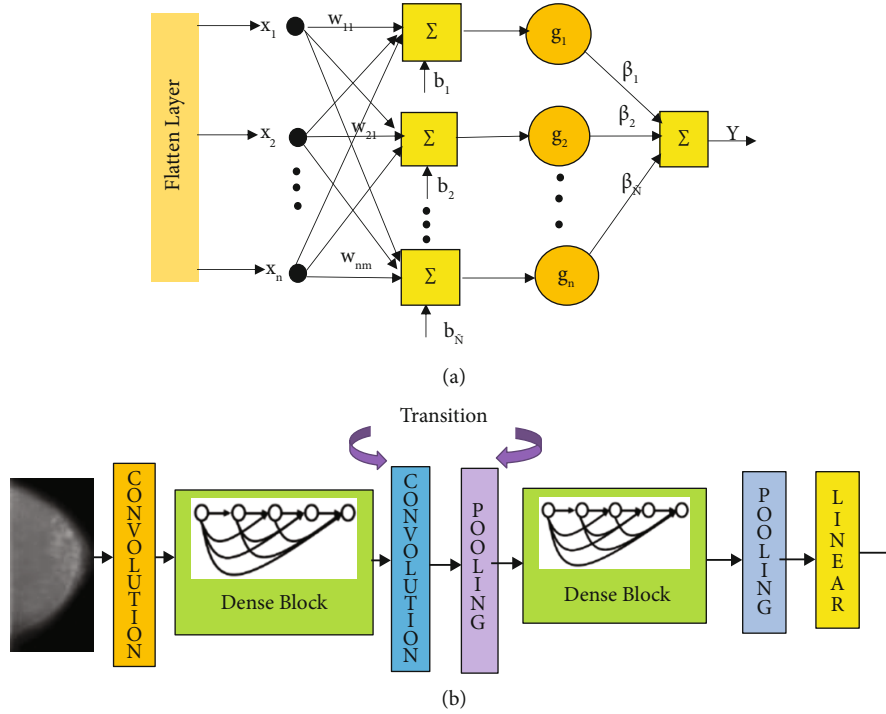


FIGURE 2: (a) ELM fully connected layer network structure. (b) DenseNet121 architecture.

Where  $H$  is the hidden layer matrix, whose matrix elements are mentioned as

$$H = \begin{bmatrix} 1 & g(w_1; x_1) & \cdots & g_N(w_N; x_1) \\ \vdots & \vdots & \vdots & \vdots \\ 1 & g(w_1; x_N) & \cdots & g_N(w_N; x_N) \end{bmatrix}. \quad (3)$$

Equation (2) is a linear system, which is given by

$$\begin{aligned} \beta &= H^\dagger y, \\ H^\dagger &= (H^T H)^{-1} H^T, \end{aligned} \quad (4)$$

where  $H^\dagger$  is the ‘‘Moore–Penrose generalized inverse of matrix  $H$ .’’ The input  $x$  is treated as the feature input dataset, which is collected from the flattened layer, and fed as input to the ELM model.

The DenseNet121 model has one  $7 \times 7$  convolution, 58 (fifty-eight)  $3 \times 3$  convolutions, 61 (sixty-one)  $1 \times 1$  convolution, 4 average pooling, and one fully connected layer. Features are extracted from dense blocks that go through transition. One  $1 \times 1$  convolutional layer and one  $2 \times 2$  average pooling layer with a stride of 2 are present in each individual transition layer. In this study, the classification performance of mammography images was improved and differentiated only by combining the DenseNet121 model with the extreme learning model. The feed-forward neural network known as the extreme learning machine serves as a classifier at the fully connected layer. We have replaced the neural network with ELM at the fully connected layer in the DenseNet121 model. The DenseNet121+ELM model’s

weights have been optimized using the AdaGrad optimization technique. The architecture model of ELM is presented in Figure 2(a). For batch size 128, the classification performance results are shown in Table 1.

**3.2.2. The Steps for Algorithm Is Presented as Follows.** In actual practice, the CNN weights are optimized with a backpropagation algorithm. The weights of the DenseNet121 model are optimized with a backpropagation algorithm. We have considered AdaGrad optimizer for our research.

*Step 1.* The input size images  $224 \times 224$  are considered for this research. The images have undergone the process of data augmentation, and the augmented images are fed as input to the models. The convolution takes place with the image and the filter. Considering the image size as  $I_{mP1 \times P2}$  is the real image; the filter is chosen randomly as the image size as  $W_{M \times N}$  filter. The convolution is given by  $[T_{M \times N}] = [I_{mP1 \times P2} * W_{M \times N}]$ .

$$[W_{ij}] = \begin{bmatrix} w_{11} & w_{12} & \cdots & w_{M-2,N} \\ w_{21} & w_{22} & \cdots & w_{M-1,N} \\ \vdots & \vdots & \cdots & \vdots \\ w_{M,N-2} & w_{M,N-1} & \cdots & w_{MN} \end{bmatrix}, \quad (5)$$

where  $i = 0, 1 \dots \dots m$  and  $j = 0, 1 \dots \dots N$ .

By rotating the filter in 180 degrees, then take transpose, We have

$$[W_{ij}]^T = [w_{11}, w_{12}, \dots, w_{21}, w_{22}, \dots \dots W_{MN}]. \quad (6)$$



TABLE 1: Comparison accuracies for proposed work and previous research.

Reference	Dataset used	Model	Accuracy in %
Abunasser et al., [14]	Kaggle	Xception	98.59%
Houssein et al., [15]	DDSM	IMPA-ResNet50	98.32%
Nawaz et al., [16]	BreakHis dataset	DenseNet	95.4%
Khan et al., [17]	CBIS-DDSM	ResNet50	88%
Hameed et al., [18]	MIFLUDAN project	Xception	97.33%
Joseph et al., [19]	BreakHis dataset	DNN	96.84%
Alkassar et al., [20]	BreakHis	DenseNet and Xception	99%
Our proposed method	Kaggle dataset	DenseNet121+ELM	99.47%

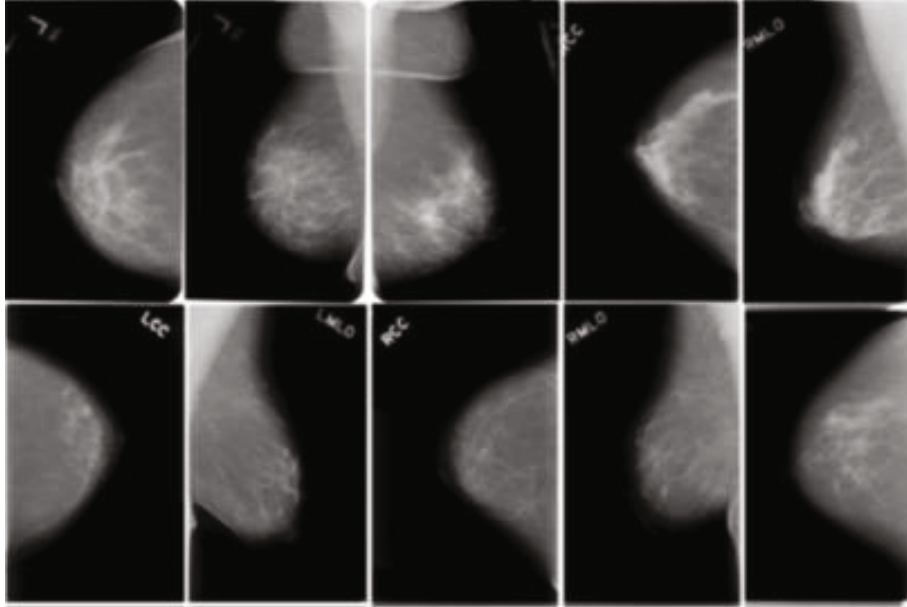


FIGURE 3: Sample images from dataset (DDSM).

TABLE 2: Image generation after data augmentation.

Type of breast images	Training	Testing
Healthy	1540	660
Nonhealthy	6160	2640
<b>Total</b>	<b>7700</b>	<b>3300</b>
<b>Total images: 11,000</b>		

*Step 2.* After convolution, it passes the phases of dense layer, and the average pooling has been accomplished with pool size (2,2) with stride 2.

*Step 3.* After average pooling, the features are flattened by the flatten layer, making the feature matrix into a vector matrix. The vector matrix is fed as input to the fully connected ELM layer. The weights are updated with AdaGrad and the learning rate was adjusted.

The updated formulae are as follows:

Now, the new weight optimization equation is given by

$$W_{ij}^{\text{new}}(n+1) = W_{ij}(n) + \eta xg(n). \quad (7)$$

TABLE 3: Training phase parameters.

Hyperparameters	Values
Image size	224 × 224
Batch size	32,64,128
Learning rate	0.0001
Rotation	45
No. of iterations	100

The learning parameter value of 0.001 is chosen for  $\eta$ . Now, the flattened vector is given.

We have

$$[F_{ij}] = [f_{11}, f_{12}, \dots, f_{21}, f_{22}, \dots, f_{MN}], \quad (8)$$

where  $i = 1, 2, \dots, M$ , and  $j = 1, 2, \dots, N$  and  $f_{11} = w_{11}^{\text{new}}, f_{12} = w_{12}^{\text{new}}, \dots, f_{MN} = w_{MN}^{\text{new}}$ .

*Step 4.* The output of the fully connected layer is passed through the softmax layer to classify the images into cancerous and noncancerous.

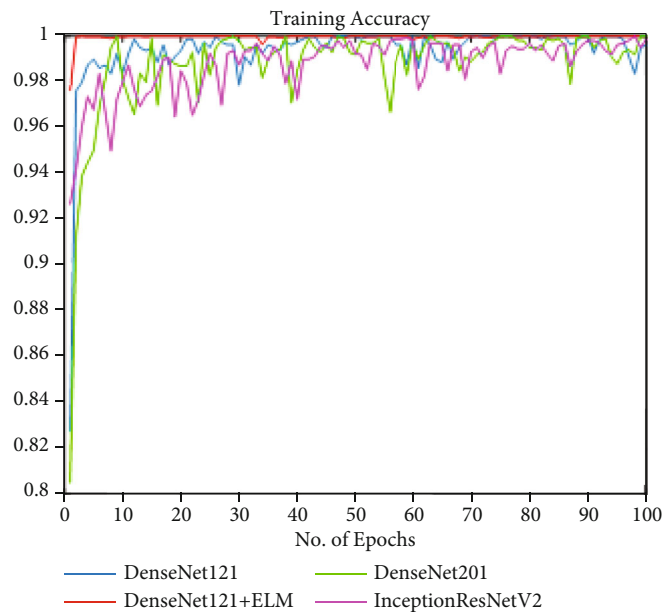


FIGURE 4: Batch size 32 training accuracy of breast cancer classification using DenseNet121, DenseNet201, InceptionResNetV2, and DenseNet121+ELM.

TABLE 4: Performance measure results of the models with batch size 32.

Models	No. of iteration	Specificity	Sensitivity	Training accuracy	Testing accuracy	Computational time in minutes
VGG19	100	97.73	97.98	94.74	90.44	219.8159
MobileNet	100	98.53	98.4	95.08	91.55	210.7027
Xception	100	98.85	98.8	95.76	93.04	199.8891
ResNet50V2	100	98.56	98.37	96.06	93.47	198.8683
InceptionV3	100	100	99.52	96.4	94.44	194.7695
InceptionResNetV2	100	98.59	100	96.8	95.31	178.7057
DenseNet201	100	98.59	99.28	97.4	96.3	174.9159
DenseNet121	100	99.27	100	97.52	96.77	171.9848
DenseNet121+ELM	100	99.37	99.94	98.67	97.33	167.3545

The output of the hidden layer is given by  $Y$  as

$$[y] = \text{sigmoid}\left(\sum f_{M1 \times N2} * [W_{M1 \times N2}^{FC}]^T\right), \quad (9)$$

where  $f_{M1 \times N2}$  is the feature matrix. Now, the  $Y$  is passed through the softmax layer, and the equation is given by

$$[C_{\text{class}}] = \text{Soft max}(y), \quad (10)$$

where

$$[C_{\text{class}}] = \begin{bmatrix} C_{\text{class1}} \\ C_{\text{class2}} \end{bmatrix} \quad (11)$$

is the output class for cancerous and noncancerous cancer.

**3.3. Dataset.** This study collects data from open-source websites using the Digital Database for Screening Mammography (DDSM) dataset [17] shown in Figure 3 and uses

classification models to compare the accuracy. The dataset is available at <https://www.kaggle.com/datasets/awsaf49/cbis-ddsm-breast-cancer-image-dataset>.

**3.4. Data Augmentation.** The data augmentation process has undergone “shifting, rotating, and flipping.” A total of 3672 images went through the data augmentation phase, generating about 11000 images. Table 2 shows that out of the total data, 70% of the images are used for training and 30% are used for testing. Table 3 lists the hyperparameters that were applied during the experiment.

## 4. Results

**4.1. Classification Results.** For training and testing, 11000 images were used during classification, and the details of image distributions are provided in Table 2. The training accuracy of DenseNet121, DenseNet201, InceptionResNetV2, and DenseNet121+ELM is compared in Figure 4. Table 4

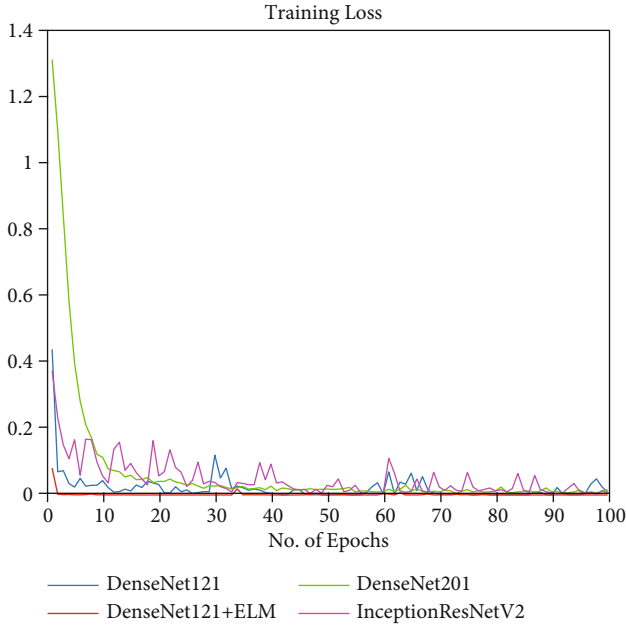


FIGURE 5: Batch size 32 training loss of breast cancer classification using DenseNet121, DenseNet201, InceptionResNetV2, and DenseNet121+ELM.

compares training accuracy for DenseNet121+ELM to the other listed models and shows that it performs better.

For batch size 32, the performance results are shown in Table 1. Figures 4 and 5 show the training accuracy and training loss for a batch size of 32. It has been found that the proposed DenseNet121+ELM model experiences less training loss than the DenseNet121, DenseNet201, and InceptionResNetV2 models. The suggested DenseNet121+ELM converged in about 20 iterations compared to almost 50, 75, and 84 iterations for DenseNet121, DenseNet201, and InceptionResNetV2, respectively.

The training accuracy and loss for the 64 batch size are shown in Figures 6 and 7. It has been noted that while DenseNet121, DenseNet201, and InceptionResNetV2 required roughly 40, 60, and 72 iterations, respectively; for convergence, the proposed DenseNet121+ELM required just about 15 iterations. When compared to the other specified models, it is found that the proposed DenseNet121+ELM model has a lower training loss. For batch size 64, the performance results are shown in Table 5.

The training accuracy and loss for a batch size of 128 are shown in Figures 8 and 9. It has been noted that the proposed DenseNet121+ELM required just about 15 iterations to reach convergence, compared to almost 20 iterations, 25 iterations, and 45 iterations for DenseNet121, DenseNet201, and InceptionResNetV2, respectively. When compared to the other models, it is observed that DenseNet201 has a higher training loss, whereas the proposed DenseNet121+ELM model has a lower training loss. The proposed DenseNet121+ELM model took lesser computational time of 159.7731 minutes, compared to 167.1242 minutes for DenseNet121, 164.3344 minutes for DenseNet201, and 160.4033 minutes for InceptionResNetV2. For batch size 128, the performance results are shown in Table 6. The sys-

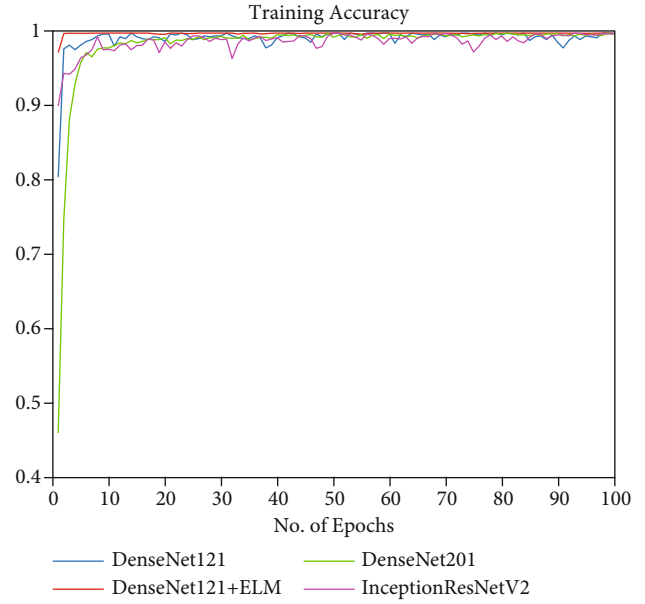


FIGURE 6: Batch size 64 training accuracy of breast cancer classification using DenseNet121, DenseNet201, InceptionResNetV2, and DenseNet121+ELM.

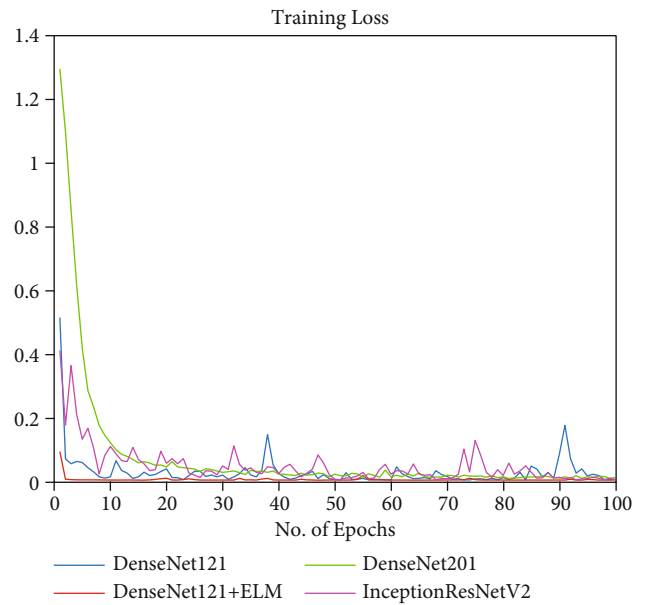


FIGURE 7: Batch size 64 training loss of breast cancer classification using DenseNet121, DenseNet201, InceptionResNetV2, and DenseNet121+ELM.

tem's performance parameters, such as "sensitivity, specificity, and accuracy," are also crucial [12] for classification.

$$\begin{aligned}
 \text{Sensitivity} &= \frac{TP}{TP + FN}, \\
 \text{Specificity} &= \frac{TN}{TN + FP}, \\
 \text{Accuracy} &= \frac{TP + TN}{TP + TN + FP + FN},
 \end{aligned} \tag{12}$$



TABLE 5: Performance measure results of the models with batch size 64.

Models	No. of iteration	Specificity	Sensitivity	Training accuracy	Testing accuracy	Computational time in minutes
VGG19	100	97.81	98.05	94.63	91.64	214.3589
MobileNet	100	98.61	98.47	94.97	92.75	202.2457
Xception	100	98.93	98.87	95.65	94.24	198.3321
ResNet50V2	100	98.64	98.44	95.95	94.67	197.3123
InceptionV3	100	100	99.57	96.29	95.64	187.3125
InceptionResNetV2	100	98.67	100	96.69	96.51	171.2487
DenseNet201	100	98.67	99.35	97.29	97.5	168.4589
DenseNet121	100	99.35	100	98.41	97.97	164.5278
DenseNet121+ELM	100	99.45	100	99.34	98.53	<b>163.8975</b>

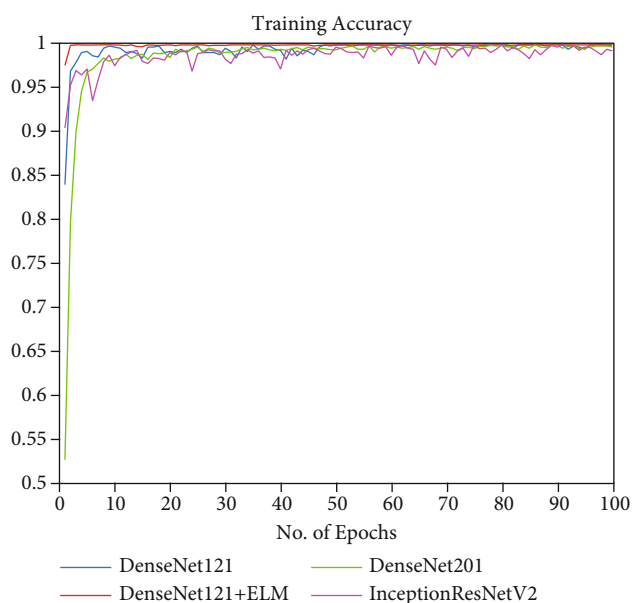


FIGURE 8: Batch size 128 training loss of breast cancer classification using DenseNet121, DenseNet201, InceptionResNetV2, and DenseNet121+ELM.

where “true positive,” “true negative,” “false positive,” and “false negative” are denoted by TP, TN, FP, and FN. We also took into account computational time, which is a crucial performance measure.

From Table 6, it can be shown that the 128 batch size leads to improved training and testing accuracy as well as faster calculation. The batch size of 128 resulted in 99.34% training accuracy, 98.84% testing accuracy, and a calculation time of 159.7731 minutes. The computation took 167.3545 minutes for batch size 32 and 163.8975 minutes for batch size 64, as shown in Tables 5 and 6, respectively. The testing accuracy is a crucial performance indicator that gives the models credibility, regardless of how well they were trained. Compared to the previous models, the suggested DenseNet121+ELM model suffers less loss. The proposed model converged in a substantially less number of epochs when compared to the total number of epochs. Table 1 shows the proposed model’s accuracy in comparison to earlier research. It can be concluded that the proposed DenseNet121+ELM model shows better performance results with

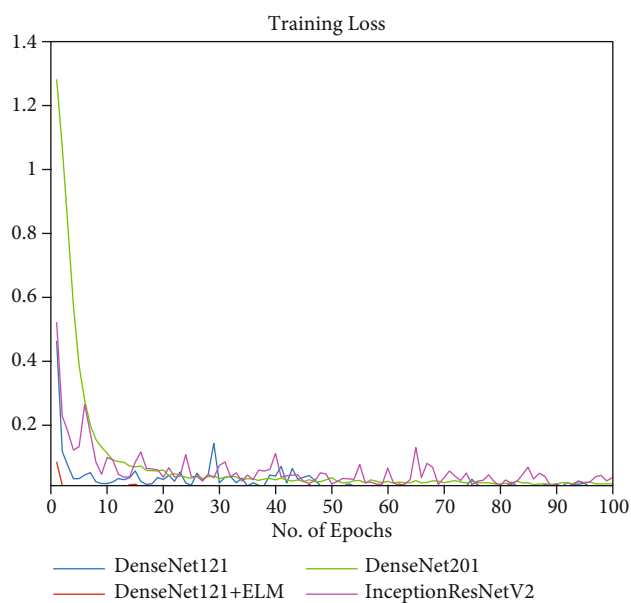


FIGURE 9: Batch size 64 training loss of breast cancer classification using DenseNet121, DenseNet201, InceptionResNetV2, and DenseNet121+ELM.

batch size 128 when compared to the other batch sizes 32 and 64. Figure 10 presents the comparison of all the models considered for the research.

## 5. Discussion

The classification procedure took into account a total of 11000 images, out of which 7700 were used for training and 3300 for testing. Table 4 gives more information about the augmented images. The VGG19, MobileNet, MobileNetV2, Xception, ResNet50V2, InceptionV3, InceptionResNetV2, DenseNet201, DenseNet121, and DenseNet121+ELM models were employed to classify the augmented images. The fully connected layer weights of the CNN models were tuned using the AdaGrad algorithm. The training performance of the malignant and noncancerous classification of breast cancer was shown in Figures 4, 6, and 8. With batch sizes of 32, 64, and 128, all the mentioned models were considered for the classification along with the proposed DenseNet121+ELM model. The training losses

TABLE 6: Performance measure results of the models with batch size 128.

Models	No. of iteration	Specificity	Sensitivity	Training accuracy	Testing accuracy	Computational time in minutes
VGG19	100	97.73	97.98	97.76	97.88	211.2344
MobileNet	100	98.53	98.41	98.23	98.42	198.1212
Xception	100	98.65	98.82	98.85	98.73	194.2076
ResNet50V2	100	98.56	98.87	98.76	98.37	193.1878
InceptionV3	100	100	99.52	98.63	98.52	183.1881
InceptionResNetV2	100	98.59	100	98.58	98.47	167.1242
DenseNet201	100	98.84	99.28	98.98	98.85	164.3344
DenseNet121	100	99.18	100	99.27	98.84	160.4033
DenseNet121+ELM	100	99.37	99.94	99.47	99.14	159.7731

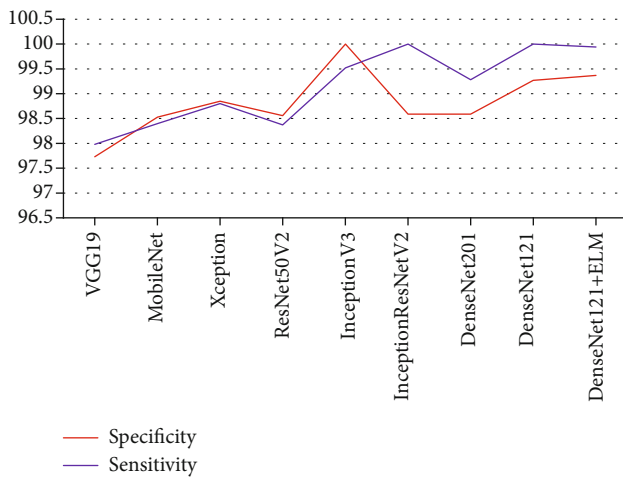


FIGURE 10: Batch size 128 specificity and sensitivity comparison of all models.

for InceptionResNetV2, DenseNet201, DenseNet121, and DenseNet121+ELM were shown in Figures 5, 7, and 9. With a batch size of 128, the VGG19 model achieved training and testing accuracy of 97.76% and 97.98%, respectively. Additionally, the VGG19 model achieved specificity, sensitivity, and computational time at corresponding values of 97.73%, 97.88%, and 211.2344 minutes. The MobileNet model achieved training and testing accuracy of 98.23% and 98.42% with a batch size of 128. Additionally, it achieved 98.53% specificity, 98.41% sensitivity, and 198.1212 minutes of computational time, respectively. The Xception model achieved 98.85% and 98.73% training and testing accuracy, and 98.65% specificity, 98.82% sensitivity, and 194.2076 minutes of processing time. The ResNet50V2 model achieved training and testing accuracy of 98.56%, 98.87%, respectively, and took 193.1878 minutes computational time for convergence. The InceptionV3 model reached training and testing accuracy of 98.63% and 98.52%, respectively. Additionally, it achieved 100% specificity, 99.52% sensitivity, and 183.1881 minutes of processing time, respectively. The InceptionResNetV2 model achieved 98.58% training and 98.47% testing accuracy, and also achieved 98.59% specificity, 100% sensitivity, with a computational time of 167.1242 minutes. The DenseNet201 model achieved training and testing accuracy of 98.98% and 98.85%, 98.84%

specificity, 99.28% sensitivity, and a computational time of 164.3344 minutes. The training and testing accuracy of 99.27% and 98.84% were achieved by the DenseNet121 model. Also, 99.18% specificity, 100% sensitivity, and a computation time of 160.4033 minutes were achieved by the model. The training and testing accuracy for the DenseNet121+ELM model were 99.47% and 99.14%, respectively. Further, 99.37% specificity, 99.94% sensitivity, and 159.7731 minutes of computational time were obtained, respectively, by the proposed DenseNet121+ELM model. For this study, training and testing data for all models with batch sizes of 34 and 64 were presented in Tables 5 and 6.100 epochs were taken into account for all categorization performance measure studies. The DenseNet121+ELM model has been proven to be suitable and worthy for classifying breast cancer.

## 6. Conclusion

In this study, a novel DenseNet121+ELM model was proposed for classifying breast cancer from mammography images. The ELM model took the role of the conventional neural network in the fully connected layer of the proposed DenseNet121+ELM model. The preprocessed images underwent data augmentation, and the aligned-augmented images served as the classification input. The DenseNet121+ELM model received the augmented images for classification. For weight optimization, the AdaGrad optimization was taken into account. The DDSM high-resolution breast-imaging dataset was considered for the classification. We have considered InceptionResNetV2, DenseNet201, DenseNet121, and DenseNet121+ELM models for figure illustration. The batch sizes 32, 64, and 128, and the learning rate of 0.001, were considered for this study. In comparison to the other models, the DenseNet121+ELM model converges faster during training and testing. The proposed DenseNet121+ELM model was considered as a reliable classifier in classifying cancerous and noncancerous breast cancer from the images. Compared to other CNN conventional algorithms, the proposed DenseNet121+ELM model will aid medical professionals and radiologists in recognizing breast cancer without needing manual interventions. The proposed DenseNet121+ELM model took lots of time to simulate, which is the model's drawback. However, this

proposed model will provide a superior solution to medical diagnosis due to the faster processing unit. This model is new, and till now, it has not been utilized elsewhere. The proposed DenseNet121+ELM model can be employed for a brain tumor dataset, liver disease dataset, etc. in future research.

## Data Availability

The dataset is collected from the publically available website <https://www.kaggle.com/datasets/awsaf49/cbis-ddsm-breast-cancer-image-dataset>.

## Conflicts of Interest

The authors of the paper Satyasis Mishra, Raj Kumar Pattnaik, Mohammed Siddique, Sunita Satapathy, and Tiruveedula Gopikrishna declare no conflict of interest or financial conflicts.

## Authors' Contributions

Satyasis Mishra prepared the documentation and methodology part of the research. Raj Kumar Pattnaik prepared the document per the journal format and helped collect and pre-process the data. Mohammed Siddique compiled research diagram, and python programs were compiled. Sunita Satapathy collected data from different parts of Ethiopia. Tiruveedula Gopikrishna prepared all simulation works and all figures with the GPU system. All authors reviewed the manuscript.

## Acknowledgments

The authors thank Dr. Mohammed Naimuddin for the critical reading of the manuscript and language editing.

## References

- [1] <https://www.cancer.org/research/cancer-facts-statistics/all-cancer-facts-figures/cancer-facts-figures-2022.html>.
- [2] D. Shen, G. Wu, and H. I. Suk, "Deep learning in medical image analysis," *Annual Review of Biomedical Engineering*, vol. 19, no. 1, pp. 221–248, 2017.
- [3] G. Andrew, M. Z. Howard, B. Chen et al., "MobileNets: efficient convolutional neural networks for mobile vision applications," 2017, arXiv:1704.04861v1 [cs.CV].
- [4] S. Xie, R. B. Girshick, P. Dollár, Z. Tu, and K. He, "Aggregated residual transformations for deep neural networks," in *2017 IEEE Conference on Computer Vision and Pattern Recognition (CVPR)*, Honolulu, HI, USA, 2016.
- [5] L. G. Falconi, M. Perez, W. G. Aguilar, and A. Conci, "Transfer learning and fine tuning in breast mammogram abnormalities classification on CBIS-DDSM database," *Advances in Science, Technology and Engineering Systems Journal*, vol. 5, no. 2, pp. 154–165, 2020.
- [6] X. Li, X. Shen, Y. Zhou, X. Wang, and T. Q. Li, "Classification of breast cancer histopathological images using interleaved DenseNet with SENet (IDSNet)," *PLoS One*, vol. 15, no. 5, article e0232127, 2020.
- [7] Y. Wang, E. J. Choi, Y. Choi, H. Zhang, G. Y. Jin, and S. B. Ko, "Breast cancer classification in automated breast ultrasound using multiview convolutional neural network with transfer learning," *Ultrasound in Medicine & Biology*, vol. 46, no. 5, pp. 1119–1132, 2020.
- [8] H. Shin, H. R. Chang, G. Roth et al., "Deep convolutional neural networks for computer-aided detection: CNN architectures, dataset characteristics and transfer learning," *IEEE Transactions on Medical Imaging*, vol. 35, no. 5, pp. 1285–1298, 2016.
- [9] C. Zhu, F. Song, Y. Wang, H. Dong, Y. Guo, and J. Liu, "Breast cancer histopathology image classification through assembling multiple compact CNNs," *BMC Medical Informatics and Decision Making*, vol. 19, no. 1, p. 198, 2019.
- [10] Y. Zhou, J. Xu, Q. Liu et al., "A radiomics approach with CNN for shear-wave elastography breast tumor classification," *IEEE Transactions on Biomedical Engineering*, vol. 65, no. 9, pp. 1935–1942, 2018.
- [11] J. Y. Chiao, K. Y. Chen, K. Y. Liao, P. H. Hsieh, G. Zhang, and T. C. Huang, "Detection and classification the breast tumors using mask R-CNN on sonograms," *Medicine (Baltimore)*, vol. 98, no. 19, article e15200, 2019.
- [12] Y. Jiang, L. Chen, H. Zhang, and X. Xiao, "Breast cancer histopathological image classification using convolutional neural networks with small SE-ResNet module," *PLoS One*, vol. 14, no. 3, article e0214587, 2019.
- [13] S. U. Khan, N. Islam, Z. Jan, I. U. Din, and J. J. P. C. Rodrigues, "A novel deep learning based framework for the detection and classification of breast cancer using transfer learning," *Pattern Recognition Letters*, vol. 125, pp. 1–6, 2019.
- [14] B. S. Abunasser, M. R. J. AL-Hiealy, I. S. Zaqout, and S. S. Abu-Naser, "Breast cancer detection and classification using deep learning Xception algorithm," *International Journal of Advanced Computer Science and Applications (IJACSA)*, vol. 13, no. 7, 2022.
- [15] E. H. Houssein, M. M. Emam, and A. A. Ali, "An optimized deep learning architecture for breast cancer diagnosis based on improved marine predators algorithm," *Neural Computing and Applications*, vol. 34, no. 20, pp. 18015–18033, 2022.
- [16] M. Nawaz, A. Adel, and T. Hassan, "Multi-class breast cancer classification using deep learning convolutional neural network," *International Journal of Advanced Computer Science and Applications (IJACSA)*, vol. 9, no. 6, 2018.
- [17] M. Heenaye-Mamode Khan, N. Boodoo-Jahangeer, W. Dullull et al., "Multi-class classification of breast cancer abnormalities using deep convolutional neural network (CNN)," *PLoS One*, vol. 16, no. 8, article e0256500, 2021.
- [18] Z. Hameed, B. Garcia-Zapirain, J. J. Aguirre, and M. A. Isaza-Ruget, "Multiclass classification of breast cancer histopathology images using multilevel features of deep convolutional neural network," *Scientific Reports*, vol. 12, no. 1, p. 15600, 2022.
- [19] A. A. Joseph, M. Abdullahi, S. B. Junaidu, H. H. Ibrahim, and H. Chiroma, "Improved multi-classification of breast cancer histopathological images using handcrafted features and deep neural network (dense layer)," *Intelligent Systems with Applications*, vol. 14, p. 200066, 2022.
- [20] S. Alkassar, A. Bilal, M. A. M. Jebur, J. H. Abdullah, and J. A. Al-Khalidy, "Going deeper: magnification-invariant approach for breast cancer classification using histopathological images," *IET Computer Vision*, vol. 15, no. 2, pp. 151–164, 2021.

- [21] A. Altameem, C. Mahanty, R. C. Poonia, A. K. J. Saudagar, and R. Kumar, "Breast cancer detection in mammography images using deep convolutional neural networks and fuzzy ensemble modeling techniques," *Diagnostics*, vol. 12, no. 8, p. 1812, 2022.
- [22] S. M. Alqhtani, "BreastCNN: a novel layer-based convolutional neural network for breast cancer diagnosis in DMR-thermogram images," *Applied Artificial Intelligence*, vol. 36, no. 1, 2022.
- [23] H. A. Hosni Mahmoud, A. H. Alharbi, and S. Doaa, "Breast cancer classification using deep convolution neural network with transfer learning," *Intelligent Automation and Soft Computing*, vol. 29, no. 3, pp. 803–814, 2021.
- [24] M. M. Altaf and National Center for Robotics Technology and Internet of Things, King Abdulaziz City for Science and Technology, Riyadh, Saudi Arabia, "A hybrid deep learning model for breast cancer diagnosis based on transfer learning and pulse-coupled neural networks," *Mathematical Biosciences and Engineering*, vol. 18, no. 5, pp. 5029–5046, 2021.
- [25] H. Aljuaid, N. Alturki, N. Alsubaie, L. Cavallaro, and A. Liotta, "Computer-aided diagnosis for breast cancer classification using deep neural networks and transfer learning," *Computer Methods and Programs in Biomedicine*, vol. 223, p. 106951, 2022.
- [26] W. M. Salama and M. H. Aly, "Deep learning in mammography images segmentation and classification: automated CNN approach," *Alexandria Engineering Journal*, vol. 60, pp. 4701–4709, 2021.
- [27] A. Jaiswal, N. Gianchandani, D. Singh, V. Kumar, and M. Kaur, "Classification of the COVID-19 infected patients using DenseNet201 based deep transfer learning," *Journal of Biomolecular Structure and Dynamics*, vol. 39, no. 15, pp. 5682–5689, 2021.
- [28] M. Rahimzadeh and A. Attar, "A modified deep convolutional neural network for detecting COVID-19 and pneumonia from chest X-ray images based on the concatenation of Xception and ResNet50V2," *Informatics in Medicine Unlocked*, vol. 19, p. 100360, 2020.
- [29] H. Gao, Z. Liu, L. van der Maaten, and K. Weinberger, "Densely connected convolutional networks," in *2017 IEEE Conference on Computer Vision and Pattern Recognition (CVPR)*, Honolulu, HI, USA, 2017.